doi:10.3788/gzxb20144307.0706015

基于十倍光学拉伸的 5 GHz 微波信号模数转换研究

彭迪,张旨遥,杨帆,袁飞,刘永
(电子薄膜与集成器件国家重点实验室 电子科技大学 光电信息学院,成都,610054)

摘 要:利用光学时间拉伸法对微波信号进行降频处理,提高了后端电子模数转换器的有效模拟带宽和有效采样速率.设计了一套对 5 GHz 微波信号十倍降频的光学时间拉伸模数转换系统.对色散导致的信号功率损耗特性以及调制引起的谐波失真进行了理论分析和数值仿真,结果表明:当系统带宽为 5 GHz时,光学时间拉伸引入的信号噪声失真比不会劣化后续电子模数转换器的有效位数,该模数转换系统的有效模带宽可达 8 GHz,有效采样率为 200 GS/s.

关键词:模数转换器;光子学;色散;拉伸;谐波失真
中图分类号:TN792;TN29 **文献标识码**:A **文章编号**:1004-4213(2014)07-0706015-5

Demonstration of a 10-Fold Stretch-Factor Photonic Analog-to-Digital Converter For a 5 GHz Radio-Frequency Signal

PENG Di, ZHANG Zhi-yao, YANG Fan, YUAN Fei, LIU Yong
(*State Key Laboratory of Electronic Thin Films and Integrated Devices, School of Optoelectronic Information, University of Electronic Science and Technology of China, Chengdu* 610054, *China*)

Abstract: A 10-fold stretch-factor photonic Time-Stretch Analog-to-Digital Converter (TS-ADC) system for a 5 GHz radio-frequency signal is achieved. By adopting the photonic time stretch scheme to compress the bandwidth of Radio-Frequency, the effective analog bandwidth and effective sampling rate of the posterior electronic Analog-to-Digital Conversion were improved. The dispersion-induced power penalty of the stretched signal as well as the modulation-induced harmonic distortion were analyzed and simulated. The theoretical analysis and experimental results indicate that the Signal-to-Noise And Distortion ratio of the photonic time-stretch process is high enough to maintain the high effective number of bit of the posterior electronic Analog-to-Digital Conversers in the bandwidth of 0～5 GHz. In addition, the designed TS-ADC system can achieve an effective analog bandwidth of 8 GHz and an effective sampling rate of 200 GS/s.

Key words: Analog-to-Digital Conversion; Photonics; Dispertion; Stretching; Harmonic distortion
OCIS Codes: 060.0060; 060.2310; 060.2380; 060.5625

0 Introduction

Analog-to-Digital Converters (ADCs) play a crucial role in enhancing the power of the Digital Signal Processing (DSP). The demand for high-speed and high-resolution ADCs is growing very rapidly in a variety of applications, such as advanced communication and radar systems[1-2]. In conventional electronic ADCs, a multi-bit resolution over a bandwidth of multi-tens of GHz is difficult to realize due to clock jitter and settling

Foundation item: The National Basic Research Program of China (No. 2012CB315701, 2012CB315702 and 2011CB301705), the National Nature Science Foundation of China (No. 60925019, 61090393, 61205109, 61377037), the Science and Technology Innovation Team of Sichuan Province (No. 2011JTD0001), and the Fundamental Research Funds for the Central Universities (No. ZYGX2011J052)
First author: PENG Di (1988－), female, Ph. D. candidate, mainly focuses on Microwave Photonic. Email: pendydidi@126.com
Supervisor (Contact author): LIU Yong (1970－), male, professor, Ph. D. degree, mainly focuses on Photonic Communication, Integrated Optics and Microwave Photonic. Email: yongliu@uestc.edu.cn
Received: Oct. 24, 2013; **Accepted**: Dec. 29, 2013

time of the sample-and-hold circuit[3-4]. Considering the above-mentioned bottleneck of the electronic ADCs, photonic ADCs have been put forward and obtained revolutionary improvements in recent years, which can be roughly divided into four classes: photonic sampled, photonic quantized, photonic sampled and quantized, and photonic assisted[5]. Photonic ADCs generally utilize the high repetition frequency and low colck jitter of the photonic pulses, which are generated by mode-lock fiber or semiconductor laser, to sample the high-speed Radio-Frequency (RF) signal[6-8].

TS-ADC is a typical type of the photonic assisted ADC, in which the ultrahigh-bandwidth electrical signals are first stretched in the time domain using optical methods and then digitalized by a single electronic ADC (for a time-limited signal) or parallel multi ADCs (for a continuous signal)[9-11]. Thanks to the bandwidth compression in the optical domain, low-speed electronic ADCs with a high resolution can be employed in the TS-ADC system to improve its effective sampling rate while maintain its high resolution, if the signal-to-noise and distortion ratio (SINAD) of the time-stretch process is high enough. Besides the enhancement of the sampling rate, another advantage of TS-ADC scheme is the reduction of clock jitter due to the time stretch of the signal, which means a potential improvement of the effective number-of bits (ENOB) restricted by the clock jitter. Unlike the multi-channel parallel time-interleaved ADC based on Optical Time Division Multiplexing (OTDM) technique[12], each electronic ADC in the TS-ADC works at or above the Nyquist rate, which can be utilized to avoid the inter-channel mismatch problems and reduce the error due to sampling clock jitter of digitizer. Therefore, the TS-ADC is recognized as one of the most promising photonic ADC scheme.

In this paper, the theoretical model of the TS-ADC system was introduced. Then, the dispersion-induced power penalty of the stretched signal was analyzed, together with the harmonic distortion under various modulation depths. Finally, a 10-fold stretch-factor photonic TS-ADC system for a 5 GHz RF signal was designed and demonstrated.

1 Operating principle and theoretical model

1.1 Operating principle

The architecture of the photonic TS-ADC system is shown in Fig. 1. A sub-picosecond pulse, which is generated by an ultrashort optical pulse source, is transformed into a chirped optical pulse after propagating through the first spool of Dispersion Compensating Fiber (DCF). The RF signal modulates the envelope of the chirped optical pulse in a Mach-Zehnder (M-Z) intensity modulator which is biased at quadrature point. This process is the so-called "time-to-wavelength mapping". Necessarily, a polarization controller is added before the M-Z modulator. An Erbium-Doped optical Fiber Amplifier (EDFA) is placed after the M-Z modulator to enhance the power of the chirped optical pulse. After passing through the second spool of DCF, the width of the chirped optical pulse is further extended due to the dispersion effect, so does the RF signal modulated on the pulse envelope. Finally, a photodetector realizes the demodulation of the stretched RF signal and a real-time oscilloscope achieves the analog-to-digital convertion.

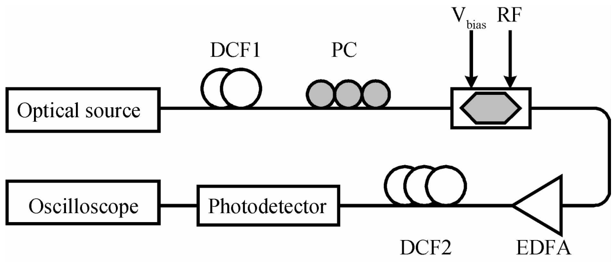

Fig. 1 Architecture of the photonic TS-ADC system

1.2 Theoretical model

Supposing the pulse generated by the optical source is an ultrashort transform-limited Gaussian one, whose optical field in the time domain and the frequency domain can be respectively written by

$$E_1(T)=E_0\exp\left(-\frac{T^2}{2T_0^2}\right) \tag{1}$$

$$E_1(\omega)=E_0\sqrt{2\pi T_0^2}\exp\left(-\frac{T_0^2\omega^2}{2}\right) \tag{2}$$

where E_0 is the amplitude of the optical field, and T_0 is the 1/e half-width of the pulse.

The propagation of the optical pulse in the two spools of DCF can be described by the generalized nonlinear Schrödinger equation (GNLSE) as follows

$$\begin{aligned}&\frac{\partial A(z,T)}{\partial z}+\frac{\alpha}{2}A(z,T)+\mathrm{j}\frac{\beta_2}{2}\frac{\partial^2 A(z,T)}{\partial T^2}-\\&\frac{\beta_3}{6}\frac{\partial^3 A(z,T)}{\partial T^3}=\mathrm{j}\gamma\{|A(z,T)|^2A(z,T)+\\&\mathrm{j}\frac{1}{\omega_0}\frac{\partial[|A(z,T)|^2A(z,T)]}{\partial T}-\\&T_R\frac{\partial[|A(z,T)|^2]}{\partial T}A(z,T)\}\end{aligned} \tag{3}$$

where A and ω_0 are the field amplitude and the central angular frequency of the optical pulse. α, β_2, β_3, γ and T_R are the loss coefficient, the Group Velocity Dispersion (GVD) coefficient, the third-order dispersion coefficient, the nonlinear coefficient and the Raman response time of the fiber.

The relationship between the output optical field E_3 and the input optical field E_2 of a push-pull M-Z modulator biased at the quadrature point is represented as

$$E_3(T)=\frac{\sqrt{2}}{2}E_2(T)\left[\cos\left(\frac{m}{2}\cos\omega_{RF}T\right)-\sin\left(\frac{m}{2}\cos\omega_{RF}T\right)\right] \tag{4}$$

where m is the modulation index and ω_{RF} is the angular frequency of the RF signal to be stretched.

The output current of the photodetector is given by

$$I(T)=\frac{1}{2}nc\varepsilon_0 A_{eff}R_{PD}E_4(T)E_4^*(T) \tag{5}$$

where E_4 is the optical field after the second spool of DCF. R_{PD} is the detector responsivity. c is the light velocity in the vaccum. ε_0 is the vacuum permittivity. n and A_{eff} are the refractive index and the effective mode area of the fiber, respectively.

2 Numerical results and discussion

Supposing that optical bandwidth is much larger than the electrical one and solely remain the GVD term in Eq. (3), the output current of the photodetector can be expressed as follows

$$\begin{aligned}I(T)=&I_{env}(T)\left[J_0^2\left(\frac{m}{2}\right)+2\sum_{n=1}^{\infty}J_n^2\left(\frac{m}{2}\right)\right]+I_{env}(T)\cdot\\&\left[-4\sum_{n=1}^{\infty}J_{2n-2}\left(\frac{m}{2}\right)J_{2n-1}\left(\frac{m}{2}\right)\cos(4n-3)\phi_{DIP}+\right.\\&\left.4\sum_{n=1}^{\infty}J_{2n-1}\left(\frac{m}{2}\right)J_{2n}\left(\frac{m}{2}\right)\cos(4n-1)\phi_{DIP}\right]\cdot\\&\cos\left(\frac{\omega_{RF}}{M}T\right)+I_{env}(T)\left[2J_1^2\left(\frac{m}{2}\right)-4\sum_{n=1}^{\infty}J_{n-1}\cdot\right.\\&\left.\left(\frac{m}{2}\right)J_{n+1}\left(\frac{m}{2}\right)\cos 4n\phi_{DIP}\right]\cos\left(\frac{2\omega_{RF}}{M}T\right)+\\&I_{env}(T)\left[-4\sum_{n=1}^{\infty}J_{2n-1}\left(\frac{m}{2}\right)J_{2n+2}\left(\frac{m}{2}\right)\cdot\right.\\&\cos(12n+3)\phi_{DIP}+4\sum_{n=1}^{\infty}J_{2n-2}\left(\frac{m}{2}\right)J_{2n+1}\left(\frac{m}{2}\right)\cdot\\&\left.\cos(12n-3)\phi_{DIP}\right]\cos\left(\frac{3\omega_{RF}}{M}T\right)+\cdots\end{aligned} \tag{6}$$

where $\phi_{DIP}=(1/2)(\beta_2 L_2/M)\omega_{RF}^2$ is the dispersion-induced phase shift, $M=(L_1+L_2)/L_1$ is the stretch factor, $L_D=T_0^2/|\beta_2|$ is the dispersion length, and the envelope function $I_{env}(T)$ is described by

$$I_{env}(T)=\frac{1}{4}nc\varepsilon_0 A_{eff}R_{PD}E_0^2\frac{1}{\sqrt{1+\left(\frac{L_1+L_2}{L_D}\right)^2}}\cdot\exp\left\{-\frac{T^2}{T_0^2\left[1+\left(\frac{L_1+L_2}{L_D}\right)^2\right]}\right\} \tag{7}$$

It can be observed from Eq. (6) that

1) The output current of the photodetector contains the pulse envelope $I_{env}(T)$ which is broadened after propagating through the two spools of DCF. Besides, each order harmonic term modulated to the envelope is also involved, whose frequency is 1/M-fold of the original one due to the time stretch.

2) In a TS-ADC system, the harmonics above (including) 2^{nd}-order are annoying as it causes distortion of the stretched signal.

3) Each harmonic possesses an inherent frequency-dependent attenuation due to the DSB modulation fact.

In our TS-ADC system, the length of the first and the second spool of DCF are 1.3 km and 11.7 km, respectively, indicating a stretch factor of $M=10$. In addition, the other relevant parameters are shown in the Table 1.

Table 1 Parameters of the light source and the dispersion compensation fiber

Physical quantity	Values and units
The central wavelength of the optical pulse	1560 nm
The full width at half maximum (FWHM) of the optial pulse	400 fs
The peak power of the optical pulse	800 W
The GVD coefficient of the DCF	-90 ps · km^{-1} · nm^{-1}
The loss coefficient of the DCF	0.6 dB · km^{-1}
The effective mode area of the DCF	5.0±1.0 μm
The relative dispersion slope of the DCF	0.0036 nm^{-1}

Fig. 2 shows the periodic power penalties of the 1^{st}-order, the 2^{nd}-order and the 3^{rd}-order harmonics, where Fig. 2 (a) and (b) are calculated for $m=0.3$ (i. e., intensity modulation depth of about 30%) and $m=\pi/2$ (i. e., intensity modulation depth of 100%), respectively. It can be seen from Fig. 2 that each harmonic attenuates periodically with the increasing RF frequency, and the high-order ($\geqslant 2^{nd}$-order) harmonic suppress ratio is low for a large intensity modulation depth. Fig. 3 and Fig. 4 give the maximum power penalty of the 1^{st}-order harmonic, and the lowest harmonic suppress ratio for the 2^{nd}-order and the 3^{rd}-order harmonics in the RF signal bandwidth of 0 ~ 5 GHz under various intensity modulation depth, respectively. It can be seen from Fig. 3 that the power penalty of the 1^{st}-order harmonic is lower than 0.02 dB in the bandwidth of 0 ~ 5 GHz for various intensity modulation depth, indicating that it has a neglectable influence on the stretched RF signal. In addition, it can be concluded from Fig. 4 that a high enough SINAD can be achieved under a proper intensity modulation depth to maintain the high resolution of the posterior electronic ADCs. For instance, the SINAD of the designed TS-ADC system should be larger than 40.3 dB, so that the ENOB can reach 6.4-bit which is the value of the commercial real-time oscilloscope of R&S_RTO1024 adopted in our experiment. Hence, the intensity modulation depth should be less than 80% in our experiment.

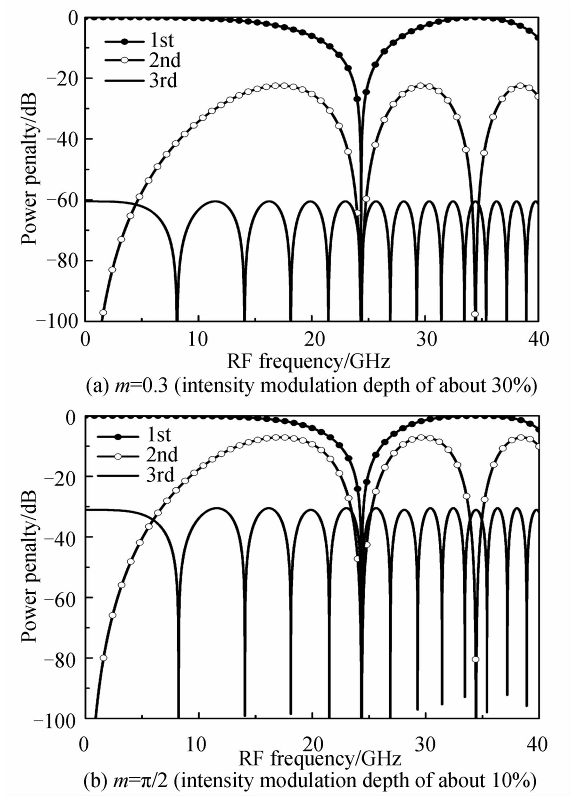

Fig. 2 The calculated dispersion-induced power penalty of each stretched harmonic component

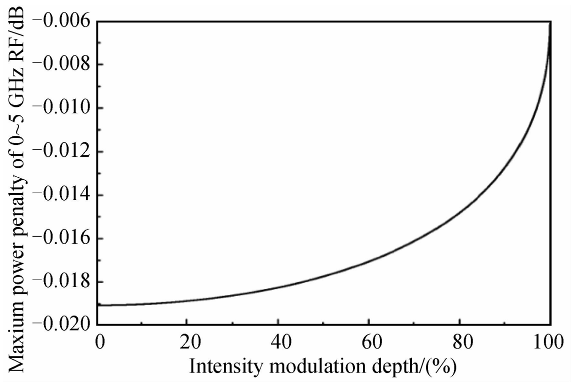

Fig. 3 The relationship between maximum power penalty and intensity modulation depth

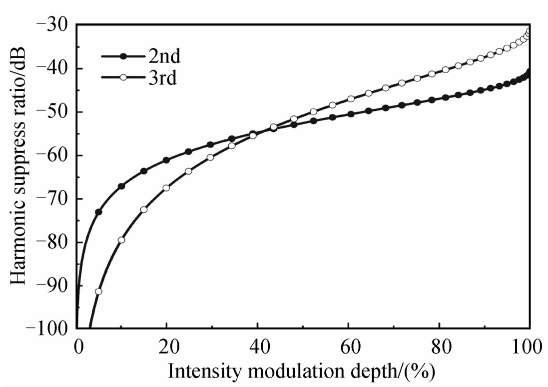

Fig. 4 The lowest harmonic suppress ratio versus intensity modulation depth

3 System simulations and experimental results

Based on the theoretical modal presented in Section 1, the simulation result of a 10-fold time stretch of a 5 GHz RF signal is presented in Fig. 5, where the parameters adopted in the simulation are given in Table I together with $m=0.3$, and the GNLSE is numerically solved using the split-step Fourier method introduced in Ref. [13]. As can be seen from the simulation results shown in Fig. 5, the designed system can achieve a good performance of a 10-fold time stretch of a 5 GHz RF signal.

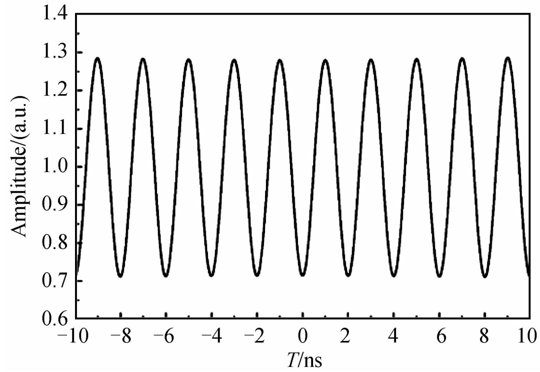

Fig. 5 The simulation result of a restored signal with original frequency of 5 GHz after removing the envelope

The real-time oscilloscope of R&S_RTO1024 with an analog bandwidth of 2 GHz and a sampling rate of 20 GS/s is employed in our experiment to act as the electronic ADC. Fig. 6 presents the experimental result of the 10-fold time stretch of a 5 GHz RF signal. The results in Fig. 2 and Fig. 6 imply that the effective analog bandwidth and the effective sampling rate of the real-time oscilloscope (R&S_RTO1024) have been enhanced to 8 GHz and 200 GS/s, respectively. Finally, it should be pointed out that the amplitude distortion of the stretched RF signal in Fig. 6 is due to the amplitude fluctuation of the home-made optical pulse source, which can be greatly reduced by employing a commercial one.

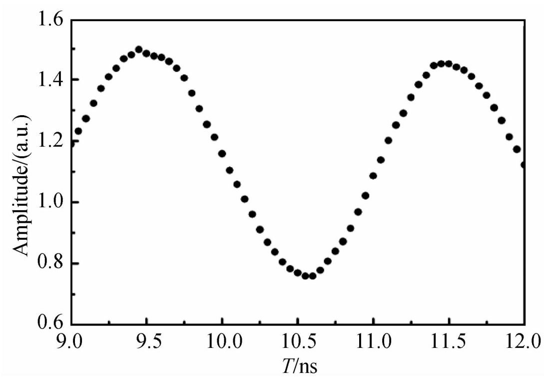

Fig. 6 The experimental result of a restored signal with original frequency of 5 GHz after removing the envelope

4 Conclusion

In summary, based on the theoretical modal of the TS-ADC system introduced in this paper, a 10-fold stretch-factor photonic analog-to-digital converter for a 5 GHz RF signal was designed. Especially, the influence of intensity modulation depth on the stretched signal distortion was analyzed in detail. Theoretical and experimental results indicate that the designed TS-ADC system can reach an effective analog bandwidth of 8 GHz and an effective sampling rate of 200 GS/s, respectively. The theoretical modal presented in this paper can be used to design photonic TS-ADC system.

Reference

[1] MURPHY J. Development of high performance analog-to-digital converters for defense applications [J]. *Computer standerds & Interfaces*, 1999, **21**(2): 98.

[2] BIN L, RONDEAU T W, REED J H, *et al*. Analog-to-digital converters[J]. *IEEE Signal Processing Magazine*, 2005, **22**(6): 69-77.

[3] HAN Yan, JALALI B. Photonic time-stretched analog-to-digital converter: fundamental concepts and practical considerations[J]. *Journal of Lightwave Technology*, 2003, **21**(12): 3085-3103.

[4] WALDEN R H. Analog-to-digital conversion in the early twenty-first century [J]. *Wiley Encyclopedia of Computer Science and Engineering*, 2008.

[5] VALLEY G C. Photonic analog-to-digital converters[J]. *Optics Express*, 2007, **15**(5): 1955-1982.

[6] ZHANG Jian-guo, LIU Yuan-shan. Development of ultra-side bandwidth all-optical sampling oscilloscope equipment[J]. *Acta Photonica Sinica*, 2011, **40**(4): 487-504.

[7] CHEN Zu-cong, RUAN Shuang-chen, GUO Chun-yu, *et al*. Passively mode-locked erbium doped fiber ring laser[J]. *Acta Photonica Sinica*, 2012, **41**(3): 267-270.

[8] DOU Yu-jie, ZHANG Hong-ming, YAO Min-yu. Ultra-short optical pulse generation based on optical frequency comb and application in optical analog-to-digital conversion[J]. *Chinese Journal of Lasers*, 2012, **39**(12): 1205006.

[9] COPPINGER F, BHUSHAN A S, JALALI B. Photonic time stretch and its application to analog-to-digital conversion[J]. *IEEE Transactions on Microwave Theory and Techniques*, 1999, **47**(7): 1309-1314.

[10] HAN Yan, JALALI B. Continuous-time time-stretched analog-to-digital converter array implemented using virtual time gating[J]. *IEEE Transactions on Circuits and Systems Ⅰ: Regular Paper*, 2005, **52**(8): 1502-1507.

[11] ASURI B, HAN Yan, JALALI B. Time-stretcheded ADC arrays[J]. *IEEE Transactions on Circuits and Systems Ⅱ: Analog to Digital Signal Processing*, 2002, **49**(7): 521-524.

[12] BLACK W C, HODGES D A. Time interleaved converter arrays[J]. *IEEE Journal of Solid-State Circuits*, 1980, **15**(6): 1022-1027.

[13] AGRAWAL G P. Nonlinear fiber optics [M]. fifth ed., Academic Press, 2012.